Journal of Natural Medicines (2022) 76:756–764
https://doi.org/10.1007/s11418-022-01623-4

ORIGINAL PAPER

Chukranoids A–I, isopimarane diterpenoids from *Chukrasia velutina*

Alfarius Eko Nugroho[1] · Masaki Tange[1] · Sumi Kusakabe[1] · Yusuke Hirasawa[1] · Osamu Shirota[2] · Michiyo Matsuno[3] · Hajime Mizukami[3] · Takahiro Tougan[4] · Toshihiro Horii[5] · Hiroshi Morita[1]

Received: 10 February 2022 / Accepted: 19 March 2022 / Published online: 5 May 2022

Abstract

Bioactivity guided separation of *Chukrasia velutina* root methanolic extract led to the isolation of nine new isopimarane diterpenoids, chukranoids A–I (**1**–**9**). The absolute configuration was then assigned by comparing the experimental CD spectra and the calculated CD spectra. Chukranoids A–I (**1**–**9**) showed moderate antimalarial activity against *Plasmodium falciparum* 3D7 strain. It seems that conjugate system in the isopimarane skeleton may influence their antimalarial activity.

Graphical abstract

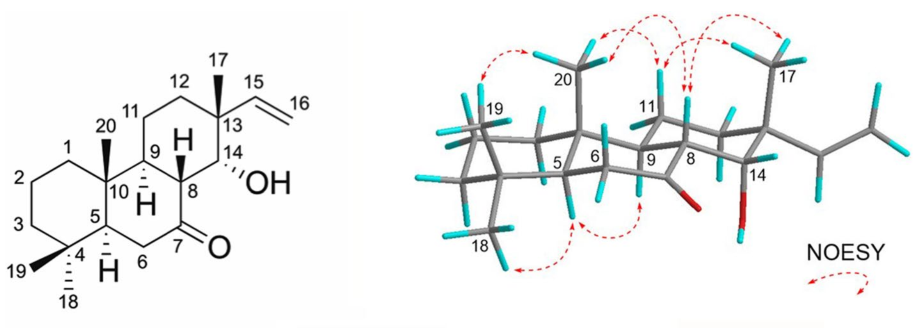

chukranoid A

Keywords Isopimarane diterpenoid · Chukranoids A–I · *Chukrasia velutina* · Meliaceae · Antimalarial activity

✉ Hiroshi Morita
moritah@hoshi.ac.jp

1 Faculty of Pharmaceutical Sciences, Hoshi University, Ebara 2-4-41, Shinagawa-ku, Tokyo 142-8501, Japan

2 Faculty of Pharmaceutical Sciences at Kagawa Campus, Tokushima Bunri University, 1314-1 Shido, Sanuki City, Kagawa 769-2193, Japan

3 The Kochi Prefectural Makino Botanical Garden, 4200-6 Godaisan, Kochi City, Kochi 781-8125, Japan

4 Research Center for Infectious Disease Control, Research Institute for Microbial Diseases, Osaka University, 3-1 Yamadaoka, Suita, Osaka 565-0871, Japan

5 Department of Malaria Vaccine Development, Research Institute for Microbial Diseases, Osaka University, 3-1 Yamadaoka, Suita, Osaka 565-0871, Japan

Introduction

Chukrasia velutina is a deciduous tree of the genus *Chukrasia*, a monotypic genus in the family Meliaceae. It is native to Indochina through Myanmar to Indonesia [1]. The plant is widely used in Ayurveda as an important medicinal plant and the extract has been reported to exhibit considerable antimalarial activity as well as antibacterial and antifungal activities. The plants of this genus have been reported to produce tetranor-triterpenoids, such as chukrasins A–E [2] from the woods of *C. tabularis*. Furthermore, tetranor-triterpenoids from *Chukrasia* plants have been reported to show various activity. Tabulalins B, C, and E, *D*-ring-opened phragmalin-type limonoids, chukvelutins E and F, C-15-isobutyryl 16-norphragmalin-type limonoids, and velutabularins B, D, E, and I have been reported to show

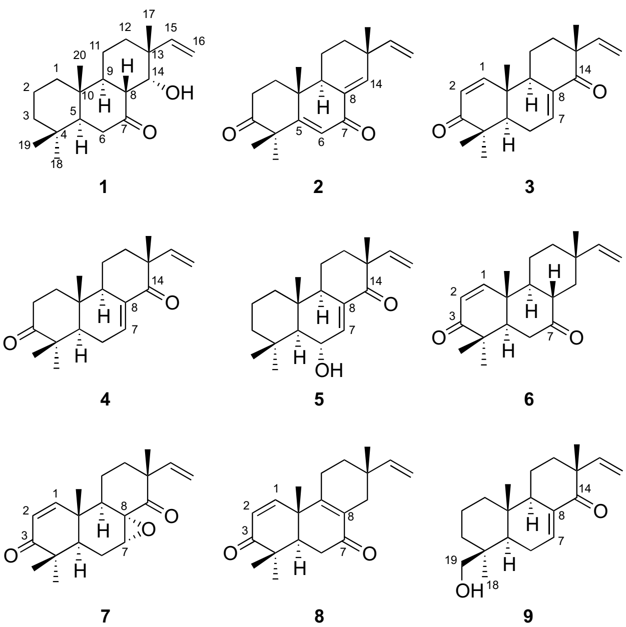

Fig. 1 Structures of **1**–**9**

inhibitory activities against LPS-induced NO production in a macrophage cell line [3–5]. On the other hand, tabulalide G exhibited moderate cytotoxic activity against MCF-7 [6].

In our search for new bioactive compounds from medicinal plants [7–19], we investigated the MeOH extract of *Chukrasia velutina* leaves which showed antimalarial activity. Bioactivity guided separation of the extract led to the isolation of nine new isopimarane diterpenoids, chukranoids A–I (**1**–**9**) (Fig. 1). Structure elucidation of **1**–**9** and the antimalarial activity of the isolated compounds are reported herein.

Results and discussion

Compound **1** was obtained as an optically active white amorphous solid. Its molecular formula of $C_{20}H_{32}O_2$ was determined by HRESIMS. IR absorptions implied the presence of ketone (1697 cm^{-1}) and hydroxy (3449 cm^{-1}) groups. The ^{1}H and ^{13}C NMR spectra (Table 1) as well as HSQC spectra implied the presence of four sp^3 methines, six sp^3 methylenes, four sp^3 methyl groups, three sp^3 quaternary carbons, one vinyl group (δ_C 147.1; δ_H 5.99, δ_C 111.7; δ_H 5.02 and 5.06), and a carbonyl group (δ_C 214.7). Among them, one sp^3 methine (δ_C 71.6; δ_H 3.98) was ascribed to that attached to an oxygen atom.

Analyses of the HSQC and ^{1}H-^{1}H COSY spectra (Fig. 2) revealed the presence of five partial structures; **a** (C-1 ~ C-3), **b** (C-5 ~ C-6), **c** (C-8, C-9, and C-14), **d** (C-11 ~ C-12), and **e** (C-15 ~ C-16). The connections between partial structures **a**–**e** were deduced mainly from the HMBC correlations of H$_3$-17, H$_3$-19, H$_3$-20 (Fig. 2). In addition, the presence of a carbonyl at C-7 and the connectivity of C-9 and C-11 were deduced from the HMBC correlations of H-6 and H-14 to C-7, and H$_2$-12 to C-9. Thus, **1** was revealed as a pimarane or isopimarane type diterpenoid.

The relative configuration of **1** was assigned by analyses of the ^{1}H-^{1}H coupling constant data and the NOESY correlations (Fig. 2). The NOESY correlations of H$_3$-20/H-8, H-11β, and H$_3$-19, H-5/H-9 and H$_3$-18, and H$_3$-17/H-8 and H-11β indicated H-8, CH$_3$-17, CH$_3$-19, and CH$_3$-20 as β-oriented, whereas H-5 and H-9 are α-oriented. Finally, H-14 was inferred to be β-oriented from the coupling constant data of H-8 (d, 12.9 Hz) and H-14 (s). Therefore, **1** (chukranoid A) was deduced to be a new isopimarane type diterpenoid.

Compound **2** was revealed to have the molecular formula $C_{20}H_{26}O_2$ by HRESIMS [m/z 321.1852 $(M+Na)^+$, $\Delta+2.1$ mmu]. The presence of two carbonyls was indicated by IR absorption bands at 1714 and 1701 cm^{-1} and conjugated system was suggested by UV absorption bands at 204 (ε 8513), 271 (ε 3725), and 311 (ε 4659) nm.

The three partial structures; **a** (C-1 ~ C-2), **b** (C-9, C-11 and C-12), and **c** (C-15 ~ C-16), which indicated by the HSQC and ^{1}H-^{1}H COSY spectra was connected by the HMBC correlations as shown in Fig. 3. The structure of **2** with three double bonds at C-5, C-8 ~ C-14, and C-15 was concluded as chukranoid B with isopimarane skeleton. The NOESY correlations between CH$_3$-20 and H-11β, CH$_3$-17 and H-11β, and CH$_3$-19 and CH$_3$-20 showed β-orientations for these protons. The similar ECD spectra at 259 (Δ ε -0.83), 309 (Δ ε -1.13) nm to **1** indicated that **2** had the same absolute structure with isopimarane skeleton as **1**.

Compound **3** was obtained as an optically active white amorphous solid. Its molecular formula of $C_{20}H_{26}O_2$ was determined by HRESIMS. The four partial structures; **a** (C-1 ~ C-2), **b** (C-5 ~ C-7), **c** (C-9, C-11 and C-12), and **d** (C-15 ~ C-16), which indicated by the HSQC and ^{1}H-^{1}H COSY spectra was connected by the HMBC correlations as shown in Fig. 4. The structure of **3** with two α,β-unsaturated ketone system at C-1 ~ C-3, and C-7, C-8 and C-14 was concluded as chukranoid C with isopimarane skeleton.

The ^{1}H and ^{13}C NMR data (Table 1) of **4** with molecular formula of $C_{20}H_{28}O_2$ were similar to **3**, suggesting their structural similarity of each other. Furthermore, the observed differences were mainly for the signals ascribed to the two adjacent methylenes (C-1 ~ C-2) in **4**. The proposed structure was further supported by the 2D NMR correlations. Based on the observed differences, the structure of **4** (chukranoid D) was concluded as shown in Fig. 1.

The molecular formula, $C_{20}H_{30}O_2$ of chukranoid E (**5**) was determined by HRESIMS. The four partial structures;

Table 1 ^{1}H and ^{13}C NMR data of **1**–**5** in $CDCl_3$

No	**1**		**2**		**3**		**4**		**5**	
	δ_H	δ_C	δ_H	δ_C	δ_H	δ_C	δ_H	δ_C	δ_H	δ_C
1a	1.10 (m)	38.6	1.91 (m)	31.4	6.96 (d, 10.4)	153.3	1.54 (ddd, 14.6, 14.0, 3.5)	37.7	1.11 (m)	38.9
1b	1.80 (m)		2.14 (ddd, 13.8, 7.6, 1.7)				2.16 (ddd, 14.0, 5.5, 3.5)		1.75 (m)	
2a	1.52 (m)	18.6	2.54 (m)	33.3	5.96 (d, 10.4)	126.3	2.31 (ddd, 14.8, 3.5, 3.5)	34.5	1.50 (m)	18.7
2b	1.59 (m)		2.67 (ddd, 19.2, 7.2, 1.7)				2.76 (ddd, 14.8, 14.6, 5.5)		1.56 (m)	
3a	1.19 (m)	41.7		214.0		203.8		215.7	1.24 (m)	43.3
3b	1.47 (m)								1.43 (m)	
4		33.6		48.1		43.8		47.3		33.2
5	1.29 (dd, 14.0, 3.4)	54.0		143.1	1.93 (m)	46.7	1.64 (m)	50.2	1.20 (d, 10.3)	56.7
6a	2.41 (dd, 14.5, 3.4)	39.7	6.75 (brs)	130.9	2.28 (2H, m)	24.1	2.25 (2H, m)	24.9	4.37 (brd, 10.3)	69.1
6b	2.31 (dd, 14.0, 14.5)									
7		214.7		183.4	7.00 (m)	137.7	6.96 (m)	137.4	6.68 (brs)	138.3
8	2.42 (d, 12.9)	50.0		142.2		109.3		108.5		108.2
9	1.68 (m)	48.4	2.53 (m)	44.5	2.40 (m)	48.5	2.21 (m)	51.7	2.23 (brd, 11.7)	52.0
10		36.5		38.0		37.5		35.1		39.2
11a	1.38 (m)	20.3	1.69 (m)	19.4	1.17 (m)	18.7	1.62 (m)	18.6	1.50 (m)	18.2
11b	1.67 (m)		1.87 (m)		1.97 (m)		1.80 (m)		1.77 (m)	
12a	1.35 (m)	28.8	1.56 (m)	33.3	1.86 (2H, m)	33.7	1.80 (m)	33.8	1.78 (m)	33.9
12b	1.80 (m)		1.65 (m)				1.87 (m)		1.86 (m)	
13		39.9		38.6		48.8		48.7		48.9
14	3.98 (s)	71.6	6.99 (m)	145.7		202.6		202.8		203.3
15	5.99 (dd, 17.5, 11.0)	147.1	5.83 (dd, 17.5, 10.7)	145.6	6.16 (dd, 17.5, 10.8)	143.2	6.17 (dd, 17.5, 11.1)	143.4	6.16 (dd, 17.7, 10.7)	143.2
16a	5.02 (d, 17.5)	111.7	5.02 (dd, 17.5, 1.1)	112.6	5.05 (d, 17.5)	113.0	5.05 (d, 17.5)	112.7	5.05 (d, 17.7)	112.8
16b	5.06 (d, 11.0)		5.04 (dd, 10.7, 1.1)		5.11 (d, 10.8)		5.11 (d, 11.1)		5.15 (d, 10.7)	
17	0.95 (3H, s)	21.7	1.17 (3H, s)	25.6	1.21 (3H, s)	24.0	1.20 (3H, s)	23.9	1.17 (3H, s)	23.6
18	0.88 (3H, s)	21.2	1.52 (3H, s)	21.8	1.14 (3H, s)	24.5	1.07 (3H, s)	24.9	1.07 (3H, s)	22.2
19	0.84 (3H, s)	32.8	1.48 (3H, s)	24.5	1.12 (3H, s)	21.6	1.14 (3H, s)	22.0	1.14 (3H, s)	36.3
20	1.08 (3H, s)	13.5	0.97 (3H, s)	19.2	1.08 (3H, s)	13.9	1.08 (3H, s)	13.6	0.90 (3H, s)	14.9

a (C-1 ~ C-3), **b** (C-5 ~ C-7) **c** (C-9, C-11 and C-12), and **d** (C-15 ~ C-16), which indicated by the HSQC and ^{1}H-^{1}H COSY spectra was connected by the HMBC correlations as shown in Fig. 4. The configuration of an oxymethine at C-6 was assigned to be β by the $^3J_{H\text{-}5/H\text{-}6}$ (10.3 Hz).

Compound **6** was revealed to have the molecular formula $C_{20}H_{28}O_2$ by HRESIMS. The ^{1}H and ^{13}C NMR data (Table 2) suggested the presence of a ketone (δ_C 210.0), an α,β-unsaturated ketone (δ_H 7.08 and δ_H 5.98; δ_C 203.4, 154.1 and 126.7), and vinyl group (δ_C 149.7; δ_H 5.81, δ_C 109.8; δ_H 4.91 and 4.99). Analyses of the 2D NMR data (Fig. 5) further supported the structure of **6**. In particular, the HMBC correlations among each partial structure **a** ~ **e** clarified the structure of the isopimarane skeleton with the above functions. The NOESY correlations also indicated the relative structure of **6** as shown in Fig. 5.

Compound **7** was obtained as an optically active white amorphous solid. Its molecular formula of $C_{20}H_{26}O_3$ was determined by HRESIMS. IR absorptions implied the presence of two ketone groups (1708 and 1675 cm^{-1}). The ^{1}H and ^{13}C NMR data (Table 2) implied the presence of an epoxy (δ_H 3.84; δ_C 59.3 and δ_C 57.8) as well as a ketone (δ_C 208.7), an α,β-unsaturated ketone (δ_H 6.81 and δ_H 5.93; δ_C 203.6, 152.1 and 126.4), and a vinyl group (δ_C 142.0; δ_H 5.98, δ_C 113.8; δ_H 5.07 and 5.12).

Analyses of the HSQC and ^{1}H-^{1}H COSY spectra (Fig. 6) revealed the presence of four partial structures; **a** ~ **d**. The HMBC correlations in Fig. 6, from which the connections between partial structures **a** ~ **d** were deduced, suggested the structure of **7** as isopimarane skeleton with the epoxy moiety at C-7 and C-8. Finally, H-7 was inferred to be β-oriented from the broad singlet peak of H-7 (δ_H 3.84). The relative configuration of **7** was assigned by analyses of the NOESY

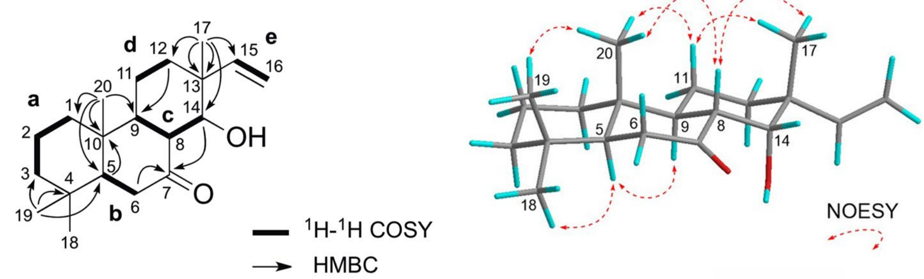

Fig. 2 Selected 2D-NMR correlations of **1**

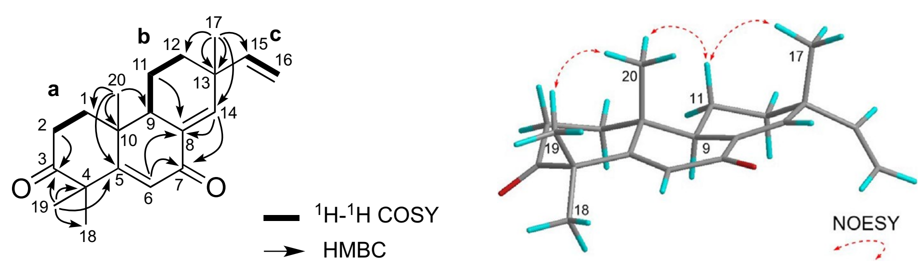

Fig. 3 Selected 2D-NMR correlations of **2**

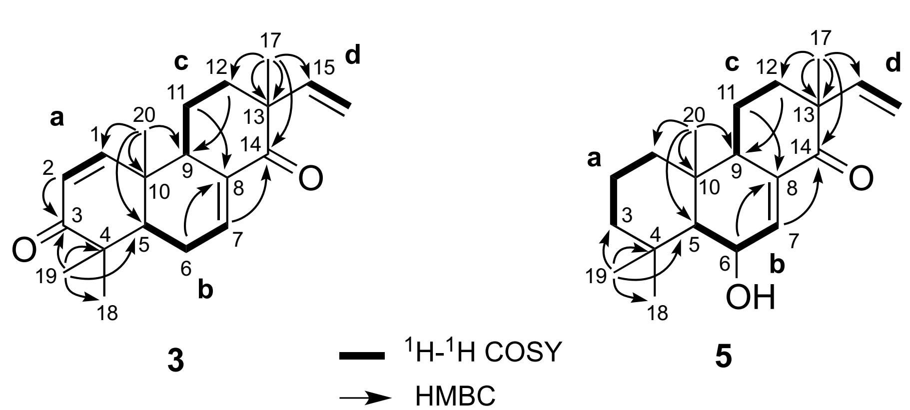

Fig. 4 Selected 2D-NMR correlations of **3** and **5**

Table 2 ^{1}H and ^{13}C NMR data of **6**–**9** in $CDCl_3$

No	**6**		**7**		**8**		**9**	
	δ_H	δ_C	δ_H	δ_C	δ_H	δ_C	δ_H	δ_C
1a	7.08 (d, 10.3)	154.1	6.81 (d, 10.3)	152.1	7.18 (d, 10.3)	151.9	1.86 (m)	38.9
1b							1.07 (m)	
2a	5.98 (d, 10.3)	126.7	5.93 (d, 10.3)	126.4	6.00 (d, 10.3)	127.3	1.50 (2H, m)	18.7
2b								
3a		203.4		203.6		202.9	1.90 (m)	35.4
3b							0.94 (m)	
4		44.5		44.0		44.0		37.8
5	2.04 (dd, 14.4, 3.0)	51.1	1.91 (m)	41.7	2.47 (dd, 12.7, 5.2)	46.6	1.40 (dd, 12.2, 5.1)	50.1
6a	2.44 (dd, 14.4, 3.0)	38.9	1.94 (m)	21.9	2.58 (m)	35.0	2.35 (m)	24.4
6b	2.53 (dd, 14.4, 14.4)		2.18 (brd, 11.7)		2.59 (m)		2.15 (m)	
7		210.0	3.84 (brs)	59.3		198.1	6.89 (m)	137.9
8	2.40 (ddd, 12.4,12.4, 3.3)	45.4		57.8		130.5		109.1
9	1.32 (m)	51.6	2.07 (m)	47.6		160.5	2.18 (m)	52.7
10		38.8		37.0		41.9		35.2
11a	1.55 (m)	21.4	1.78 (m)	18.7	2.33 (m)	24.5	1.75 (m)	18.4
11b	1.86 (m)		2.09 (m)		2.42 (m)		2.53 (m)	
12a	1.56 (m)	36.2	1.91 (m)	32.5	1.43 (m)	33.6	1.83 (m)	34.0
12b	2.23 (m)		2.07 (m)		1.69 (m)		1.77 (m)	
13		35.7		50.3		34.4		48.6
14a	1.30 (m)	36.1		208.7	2.08 (d, 17.9)	33.3		203.2
14b	1.90 (m)				2.39 (d, 17.9)			
15	5.81 (dd, 17.5, 10.7)	149.7	5.98 (dd, 17.5, 10.7)	142.0	5.66 (dd, 17.6, 10.8)	144.5	6.17 (dd, 17.7, 10.9)	143.7
16a	4.99 (d, 17.5)	109.8	5.07 (d, 17.5)	113.8	4.83 (d, 17.6)	112.1	5.04 (d, 17.7)	112.5
16b	4.91 (d, 10.7)		5.12 (d, 10.7)		4.93 (d, 10.8)		5.09 (d, 10.9)	
17	1.00 (3H, s)	21.9	1.24 (3H, s)	23.6	1.05 (3H, s)	28.1	1.16 (3H, s)	23.9
18	1.12 (3H, s)	21.5	1.13 (3H, s)	24.2	1.09 (3H, s)	25.3	0.98 (3H, s)	26.5
19a	1.14 (3H, s)	26.3	1.08 (3H, s)	22.4	1.13 (3H, s)	21.4	3.85 (d, 10.9)	64.9
19b							3.55 (d, 10.9)	
20	1.33 (3H, s)	15.5	1.10 (3H, s)	15.8	1.35 (3H, s)	22.2	0.82 (3H, s)	14.8

correlations (Fig. 6). In addition, the ^{13}C chemical shifts of C-5, C-7, and C-8 for both 7,8-α-epoxy-**7** and 7,8-β -epoxy-**7** were computed from DFT calculations using the ωB97X-D/6-31G(d) functional and basis set combination supplied with Spartan'20 software for Windows [20]. Experimental data of δ_{C5} 41.7, δ_{C7} 59.3, and δ_{C8} 57.8 were well coincident with those of the calculated values (δ_{C5} 41.7, δ_{C7} 58.1, and δ_{C8} 58.3) of 7,8-β-epoxy-**7**, when compared with those (δ_{C5} 47.7, δ_{C7} 55.7, and δ_{C8} 63.2) of 7,8-β-epoxy-**7** (Supporting information).

Compound **8** was revealed to have the molecular formula $C_{20}H_{26}O_2$ by HRESIMS. The presence of two α,β-unsaturated ketones (δ_H 7.18 and δ_H 6.00, and δ_C 202.9, 151.9 and 127.3; δ_C 198.1, 160.5 and 130.5) was indicated

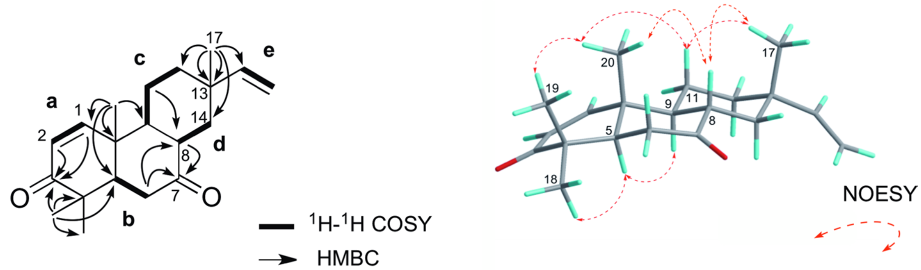

Fig. 5 Selected 2D-NMR correlations of **6**

Fig. 6 Selected 2D-NMR correlations of **7**

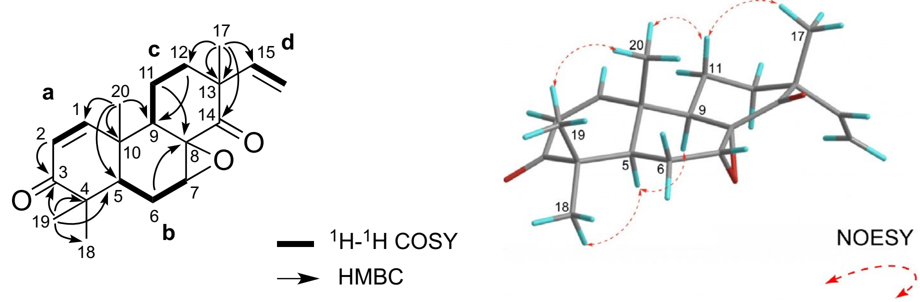

Fig. 7 Selected 2D-NMR correlations of **9**

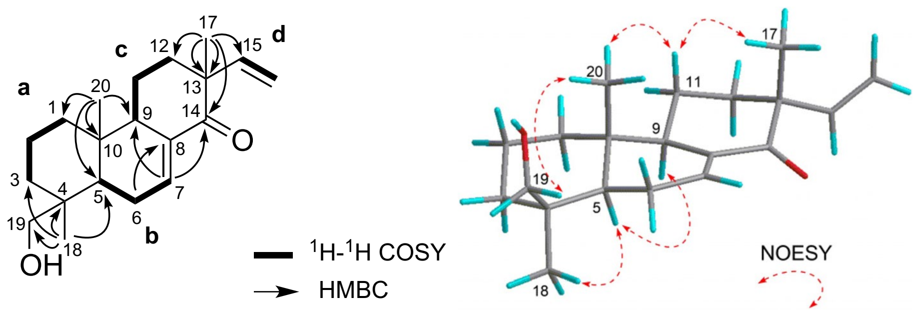

like as in **3** by ^{1}H and ^{13}C NMR data (Table 2). The conjugated positions were revealed to be C-1 ~ C-3 by the HMBC correlations of H-1 (δ_H 7.18) to C-3 (δ_C 202.9) and C-7 ~ C-9 by those of H-6 (δ_H 2.58) to C-8 (δ_C 130.5) and H-12 (δ_H 1.43) to C-9 (δ_C 160.5).

Compound **9** with the molecular formula $C_{20}H_{30}O_2$ was obtained as optically active white amorphous solids. IR absorption implied the presence of conjugated ketone (1698 cm^{-1}) and hydroxy (3421 cm^{-1}) groups. Their ^{1}H and ^{13}C NMR data (Table 2) suggested the presence of a hydroxy methyl group [δ_H 3.85 and 3.55 (each d, 10.9 Hz) δ_C 64.9]. The HMBC correlations of H-7 (δ_H 6.89) and H_3-17 to C-14 (δ_C 203.2) and H-7 to C-9 (δ_C 52.7) verified the presence of a carbonyl at C-14 and a double bond at C-7 in **9** (Fig. 7). Further structure elucidation and chemical shift assignments were done through analyses of the 2D NMR data.

The relative configuration of **9** was confirmed through analyses of the NOESY correlations as shown in Fig. 7, NMR chemical shifts, and ^{1}H-^{1}H coupling constant data. Particularly, C-17, C-19 and C-20 were deduced to be β-oriented from the NOESY correlations of H_3-20/H-19, H-11β, and H_3-17/H-11β. On the other hand, H-5 and H-9 were deduced to be α-oriented.

The absolute configuration of chukranoid C (**3**) was assigned by comparing the experimental CD spectra and the calculated CD spectra as shown in Fig. 8. CD calculation was performed by Turbomole 7.1 [21] using RI-DFT-BP86/def-TZVP level of theory on RI-DFT-BP86/def-TZVP optimized geometries. The experimental CD spectra showed similar CD pattern compared to calculated CD spectra. Therefore, the absolute configuration of **3** was proposed as shown in Fig. 1. Based on biogenetic considerations, the absolute configurations of the other chukranoids, showing the negative optical rotation around 250–300 nm, should be considered to be the same as that of **3**.

Antimalarial activity

Malaria still remains one of the leading deadliest diseases throughout the world. The emergence and spread of growing resistance to the first-line antimalarials are an alarmingly serious problem in malaria control, demanding the need for new drugs. So far, some isopimarane diterpenoids from *Platycladus orientalis* have been reported to show in vitro anti-plasmodial activity [22]. Chukranoids A–I (**1**–**9**) showed moderate antimalarial activity against *Plasmodium falciparum* 3D7 strain (Table 3). It seems that conjugate system in the isopimarane diterpenoid may influence their antimalarial activity.

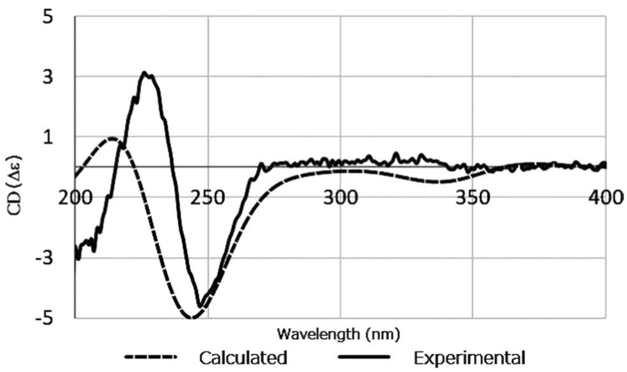

Fig. 8 Calculated and experimental CD spectra of chukranoid E (**3**)

Table 3 Antimalarial activity of **1**–**9** against *P. falciparum* 3D7 strain

	IC_{50} (μM)
1	> 50 (GI = 12.8% at 50 μM)
2	26.3
3	22.7
4	28.4
5	32.0
6	33.7
7	32.1
8	21.4
9	31.8

IC_{50}: half-maximal (50%) inhibitory concentration, *GI* : growth inhibition

Experimental section

General experimental procedures. Optical rotations were measured on a JASCO DIP-1000 polarimeter. UV spectra were recorded on a Shimadzu UVmini-1240 spectrophotometer and IR spectra on a JASCO FT/IR-4100 spectrophotometer. High-resolution ESI MS were obtained on a JMS-T100LP (JEOL). ^{1}H and 2D NMR spectra were measured on a 400 MHz or 600 MHz spectrometer at 300 K, while ^{13}C NMR spectra were on a 100 MHz or 150 MHz spectrometer. The residual solvent peaks were used as internal standards (δ_H 7.26 and δ_C 77.0 for $CDCl_3$). Merck silica gel 60 (40–63 µm) was used for the column chromatography, and the separations were monitored by Merck silica gel 60 $F_{254,}$ or Merck silica gel RP C-18 F_{254} TLC plates.

Material. The root of *C. velutina* were collected in Popa Mountain Park, Mandalay Region, Myanmar under the Memorandum of Understanding between the Kochi Prefectural Makino Botanical Garden (MBK), Japan and the Forestry Department, the Ministry of Natural Resources and Environmental Conservation, Myanmar. The botanical identification was made by Dr. Nobuyuki TanakaMBK, currently National Museum of Nature and Science. Voucher specimen (Herbarium No. MBK 0,113,430) is deposited in the Herbarium of MBK.

Extraction and isolation. The dried ground root of *Chukrasia velutina* (100 g) was extracted with MeOH, and the extract (0.96 g) was successively partitioned with *n*-hexane, EtOAc, *n*-BuOH, and water. The *n*-hexane-soluble fraction (664 mg) were separated further by a silica gel column (*n*-hexane/EtOAc, 4:1) to afford 13 fractions.

Fraction 2 was separated by a silica gel column chromatography (toluene/EtOAc, 1:0 → 9:1) to afford 7 fractions (fractions 2–1–2–7). Fractions 2–4 were separated further by an ODS column (MeOH/H_2O, 1:0 → 9:1) to afford chukranoid A (**1**, 0.6 mg, 0.0006%).

Fraction 3 was separated by a silica gel column chromatography (toluene/EtOAc, 1:0 → 9:1) to afford 13 fractions (fractions 3–1–3–13). Fractions 3–4 were separated further by an ODS column (MeOH/H_2O), and then an ODS HPLC column (COSMOSIL $5C_{18}$MSII 10 × 250 mm, 68.0% $MeOH_{(aq)}$ at 3.0 mL/min, UV detection at 210 nm) to afford chukranoids B (**2**, 1.7 mg, 0.0017%), C (**3**, 0.1 mg, 0.0001%), D (**4**, 0.3 mg, 0.0003%), and E (**5**, 1.3 mg 0.0013%).

Fraction 4 was separated by a silica gel column chromatography (toluene/EtOAc, 1:0 → 9:1) to afford 10 fractions (fractions 4–1–4–10). Fraction 4–4 was separated further by an ODS HPLC column (COSMOSIL $5C_{18}$MSII 10 × 250 mm, 68.0% $MeOH_{(aq)}$ at 3.0 mL/min, UV detection at 210 nm) to afford chukranoid F (**6**, 1.6 mg, 0.0016%, t_R 24.0 min). Fraction 4–7 was separated further by an ODS HPLC column (COSMOSIL $5C_{18}$MSII 10 × 250 mm, 68.0% $MeOH_{(aq)}$ at 3.0 mL/min, UV detection at 210 nm) to afford chukranoid G (**7**, 1.2 mg, 0.0012%, t_R 24.4 min).

Fraction 5 was separated by a silica gel column chromatography (toluene/EtOAc, 1:0 → 9:1) to afford 11 fractions (fractions 5–1–5–11). Fraction 5–6 was separated further by an ODS HPLC column (COSMOSIL $5C_{18}$MSII 10 × 250 mm, 67.0% $MeOH_{(aq)}$ at 3.0 mL/min, UV detection at 210 nm) to afford orizalexin C, and fraction 5–7 was separated by the same condition to afford chukranoid H (**8**, 0.6 mg, 0.0006%, t_R 36.0 min).

Fraction 7 was separated by a silica gel column chromatography (*n*-hexane:EtOAc, 8:2 → 1:1) to afford chukranoid I (**9**, 1.8 mg, 0.0018%).

Chukranoid A (**1**): white amorphous solid. $[\alpha]_D^{27}$ -40 (*c* 0.3, $CHCl_3$). IR (Zn-Se) ν_{max} 3449 and 1697 cm^{-1}; UV (MeOH) λ_{max} 204 (ε 8755), 268 (ε 3841), 310 (ε 4823) nm; CD (MeOH) λ_{max} 289 ($\Delta\varepsilon$ -1.82) nm; ^{1}H and ^{13}C NMR, see Table 1. ESIMS *m/z* 327 (M + Na)$^+$. HRESIMS *m/z* 327.2324 [calcd. for $C_{20}H_{32}O_2Na$ (M + Na)$^+$: 327.2300].

Chukranoid B (**2**): white amorphous solid. $[\alpha]_D^{27}$ -65 (*c* 0.9, $CHCl_3$). IR (Zn-Se) ν_{max} 1714 and 1701 cm^{-1}; UV (MeOH) λ_{max} 204 (ε 8513), 271 (ε 4659) nm; CD (MeOH) λ_{max} 259 ($\Delta\varepsilon$ -0.83), 309 ($\Delta\varepsilon$ -1.13) nm; ^{1}H and ^{13}C NMR, see Table 1. ESIMS *m/z* 321 (M + Na)$^+$. HRESIMS *m/z* 321.1852 [calcd. for $C_{20}H_{26}O_2Na$ (M + Na)$^+$: 321.1831].

Chukranoid C (**3**): white amorphous solid. $[\alpha]_D^{27}$ -34 (*c* 0.2, $CHCl_3$). IR (Zn-Se) ν_{max} 1725 and 1677 cm^{-1}; UV (MeOH) λ_{max} 204 (ε 6450), 231 (ε7637) nm; CD (MeOH) λ_{max} 231 ($\Delta\varepsilon$ 2.44), 248 ($\Delta\varepsilon$ -4.08) nm; ^{1}H and ^{13}C NMR, see Table 1. ESIMS *m/z* 321 (M + Na)$^+$. HRESIMS *m/z* 321.1861 [calcd. for $C_{20}H_{26}O_2Na$ (M + Na)$^+$: 321.1831].

Chukranoid D (**4**): white amorphous solid. $[\alpha]_D^{25}$ -11 (*c* 0.2, $CHCl_3$). IR (Zn-Se) ν_{max} 1709 and 1685 cm^{-1}; UV (MeOH) λ_{max} 203 (ε 6968), 251 (ε8310) nm; CD (MeOH) λ_{max} 247 ($\Delta\varepsilon$ -2.73) nm; ^{1}H and ^{13}C NMR, see Table 1. ESIMS *m/z* 301 (M + Na)$^+$. HRESIMS *m/z* 323.1999 [calcd. for $C_{20}H_{28}O_2Na$ (M + Na)$^+$: 323.1987].

Chukranoid E (**5**): white amorphous solid. IR (Zn-Se) ν_{max} 3566 and 1716 cm^{-1}; UV (MeOH) λ_{max} 202 (ε 7595), 239 (ε5002) nm; CD (MeOH) λ_{max} 199 ($\Delta\varepsilon$ -0.17) nm; ^{1}H and ^{13}C NMR, see Table 1. ESIMS *m/z* 325 (M + Na)$^+$. HRESIMS *m/z* 325.2163 [calcd. for $C_{20}H_{30}O_2Na$ (M + Na)$^+$: 325.2143].

Chukranoid F (**6**): white amorphous solid. IR (Zn-Se) ν_{max} 1701 and 1669 cm^{-1}; UV (MeOH) λ_{max} 203 (ε 7879), 227 (ε 9040) nm; CD (MeOH) λ_{max} 227 (Δ ε 2.04) nm; ^{1}H and ^{13}C NMR, see Table 2. ESIMS *m/z* 323 (M + Na)$^+$. HRESIMS *m/z* 323.2004 [calcd. for $C_{20}H_{28}O_2Na$ (M + Na)$^+$: 323.1987].

Chukranoid G (**7**): white amorphous solid. IR (Zn-Se) ν_{max} 1708 and 1675 cm^{-1}; UV (MeOH) λ_{max} 207 (ε 7860), 224 (ε 8028) nm; CD (MeOH) λ_{max} 228 (Δ ε 1.36) nm; ^{1}H and ^{13}C NMR, see Table 1. ESIMS *m/z* 337 (M + Na)$^+$. HRESIMS *m/z* 337.1790 [calcd. for $C_{20}H_{26}O_3Na$ (M + Na)$^+$: 337.1780].

Chukranoid H (**8**): white amorphous solid. IR (Zn-Se) ν_{max} 1709 and 1685 cm^{-1}; UV (MeOH) λ_{max} 226 (ε 8010), 243 (ε 7873) nm; CD (MeOH) λ_{max} 211 (Δ ε 3.34), 245 (Δ ε -1.71), 330 (Δ ε 0.66) nm; ^{1}H and ^{13}C NMR, see Table 1. ESIMS *m/z* 321 (M + Na)$^+$. HRESIMS *m/z* 321.1847 [calcd. for $C_{20}H_{26}O_2Na$ (M + Na)$^+$: 321.1831].

Chukranoid I (**9**): white amorphous solid. IR (Zn-Se) ν_{max} 3421 and 1698 cm^{-1}; UV (MeOH) λ_{max} 204 (ε 8480) and 244 (ε 8154) nm; CD (MeOH) λ_{max} 217 (Δ ε 1.54), 241 (Δ ε -0.43) and 334 (Δ ε 0.44) nm; ^{1}H and ^{13}C NMR, see Table 1. ESIMS *m/z* 325 (M + Na)$^+$. HRESIMS *m/z* 325.2167 [calcd. for $C_{20}H_{30}O_2Na$ (M + Na)$^+$: 325.2143].

CD calculation

The conformations were obtained using Monte Carlo analysis with MMFF94 force field and charges on Macromodel 9.1. CD calculations were performed in Turbomole 7.1 [21] using RI-DFT-BP86/def-TZVP level of theory on RI-DFT-BP86/def-TZVP optimized geometries.

Parasite strain and culture. *P. falciparum* laboratory strain 3D7 was obtained from Prof. Masatsugu Kimura (Osaka City University, Osaka, Japan). For the assessment of antimalarial activity of the compounds in vitro, the parasites were cultured in Roswell Park Memorial Institute (RPMI) 1640 medium supplemented with 0.5 g/L L-glutamine, 5.96 g/L HEPES, 2 g/L sodium bicarbonate ($NaHCO_3$), 50 mg/L hypoxanthine, 10 mg/L gentamicin, 10% heat-inactivated human serum, and red blood cells (RBCs) at a 3% hematocrit in an atmosphere of 5% CO_2, 5% O_2, and 90% N_2 at 37 °C as previously described [23]. Ring-form parasites were collected using the sorbitol synchronization technique [24]. Briefly, the cultured parasites were collected by centrifugation at 840 g for 5 min at room temperature, suspended in a fivefold volume of 5% D-sorbitol (Nacalai Tesque, Kyoto, Japan) for 10 min at room temperature, and then they were washed twice with RPMI 1640 medium to remove the D-sorbitol. The utilization of blood samples of healthy Japanese volunteers for the parasite culture was approved by the institutional review committee of the Research Institute for Microbial Diseases (RIMD), Osaka University (approval number: 22–3).

Antimalarial activity. Ring-form-synchronized parasites were cultured with compounds **1**–**9** at sequentially decreasing concentrations (50, 15, 5, 1.5, 0.5, and 0.15 μM) for 48 h. Parasitemia was measured by the flow cytometric analysis using an automated hematology analyzer, XN-30. The XN-30 analyzer was equipped with a prototype algorithm for cultured falciparum parasites (prototype; software version: 01–03, (build 16)) and used specific reagents (CELLPACK DCL, SULFOLYSER, Lysercell M, and Fluorocell M) (Sysmex, Kobe, Japan) [25, 26]. Approximately, 100 μL of the culture suspension diluted with 100 μL phosphate-buffered saline was added to a BD Microtainer MAP Microtube for Automated Process K_2 EDTA 1.0 mg tube (Becton Dickinson and Co., Franklin Lakes, NJ, USA) and loaded onto the XN-30 analyzer with an auto-sampler as described in the instrument manual (Sysmex). The parasitemia (MI-RBC%) was automatically reported [25]. Then, 0.5% DMSO alone or containing 5 μM artemisinin used as the negative and positive controls, respectively. The growth inhibition (GI) rate was calculated from the MI-RBC% according to the following equation:

$$GI(\%) = 100 - (\text{test sample} - \text{positive control}) / (negativecontrol - positivecontrol) \times 100$$

The half-maximal (50%) inhibitory concentration (IC_{50}) was calculated from GI (%) using GraphPad Prism version 9.0 (GraphPad Prism Software, San Diego, CA, USA) [27].

Supplementary Information The online version contains supplementary material available at https://doi.org/10.1007/s11418-022-01623-4.

Acknowledgements We express thanks to Prof. Masatsugu Kimura (Osaka City University, Osaka, Japan) for the kind gift of the 3D7 strain, Mr. Yuji Toya and Dr. Kinya Uchihashi (Sysmex) for the setting of the XN-30 analyzer, and Ms. Toshie Ishisaka and Ms. Sawako Itagaki for their technical assistance. We appreciate for supporting of Dr. Nyi Nyi Kyaw, Director General of the Forest Department, Myanmar to correct the plant materials in Myanmar. This work was partly supported by JSPS KAKENHI Grant Number JP19K07152 and JP 16K08309, Japan.

References

1. Mabberley DJ (2011) Meliaceae. Flowering Plants Eudicots: Sapindales, Cucurbitales, Myrtaceae. Kubitzki K, Springer**:** 185–211
2. Ragettli T, Tamm C (1978) The Chukrasines A, B, C, D and E, five new tetranortriterpenes from *Chukrasia tabularis* A. JUSS Helv Chim Acta 61:1814–1831
3. Luo J, Li Y, Wang JS, Kong LY (2011) D-Ring-opened phragmalin-type limonoids from *Chukrasia tabularis* var. *velutina*. Chem Biodivers 8:2261–2269
4. Luo J, Li Y, Wang JS, Lu J, Kong LY (2012) Three new C-15-isobutyryl 16-norphragmalin-type limonoids from *Chukrasia tabularis* var. *velutina*. Phytochem Lett 5:249–252
5. Luo J, Wang JS, Luo JG, Wang XB, Kong LY (2011) Velutabularins A-J, phragmalin-type limonoids with novel cyclic moiety from *Chukrasia tabularis* var. *velutina*. Tetrahedron 67:2942–2948
6. Luo J, Li Y, Wang JS, Wang XB, Luo JG, Kong LY (2011) Phragmalin-type limonoid orthoesters from *Chukrasia tabularis* var. *velutina*. Chem Pharm Bull 59:225–230
7. Prema, Wong CP, Kodama T, Nugroho AE, El-Desoky AH, Awouafack MD, Win YY, Ngwe H, Abe I, Morita H, Morita H (2020) Three new quassinoids isolated from the wood of *Picrasma javanica* and their anti-Vpr activities. J Nat Med 74:571–578
8. Prema, Wong CP, Awouafack MD, Nugroho AE, Win YY, Win NN, Ngwe H, Morita H, Morita H (2019) Two new quassinoids and other constituents from the *Picrasma javanica* wood and their biological activities. J Nat Med 73:589–596
9. Kaneda T, Matsumoto M, Sotozono Y, Fukami S, Nugroho AE, Hirasawa Y, Hadi AHA, Morita H (2019) Cycloartane triterpenoid (23R, 24E)-23-acetoxymangiferonic acid inhibited proliferation and migration in B16–F10 melanoma via MITF downregulation caused by inhibition of both β-catenin and c-Raf–MEK1–ERK signaling axis. J Nat Med 73:47–58
10. Tang Y, Nugroho AE, Hirasawa Y, Tougan T, Horii T, Hadi AHA, Morita H (2019) Leucophyllinines A and B, bisindole alkaloids from *Leuconotis eugeniifolia*. J Nat Med 73:533–540
11. Hirasawa Y, Dai X, Deguchi J, Hatano S, Sasaki T, Ohtsuka R, Nugroho AE, Kaneda T, Morita H (2019) New vasorelaxant indole alkaloids, taberniacins A and B, from *Tabernaemontana divaricata*. J Nat Med 73:627–632
12. Amelia P, Nugroho AE, Hirasawa Y, Kaneda T, Tougan T, Horii T, Morita H (2019) Two new sarpagine-type indole alkaloids and antimalarial activity of 16-demethoxycarbonylvoacamine from *Tabernaemontana macrocarpa* Jack. J Nat Med 73:820–825
13. Nugroho AE, Hashimoto A, Wong CP, Yokoe H, Tsubuki M, Kaneda T, Hadi AHA, Morita H (2018) Ceramicines M-P from *Chisocheton ceramicus*: isolation and structure–activity relationship study. J Nat Med 72:64–72
14. Nugroho AE, Inoue D, Wong CP, Hirasawa Y, Kaneda T, Shirota O, Hadi AHA, Morita H (2018) Reinereins A and B, new onocerane triterpenoids from *Reinwardtiodendron cinereum*. J Nat Med 72:588–592
15. Nugroho AE, Zhang W, Hirasawa Y, Tang Y, Wong CP, Kaneda T, Hadi AHA, Morita H (2018) Bisleuconothines B-D, modified eburnane–aspidosperma bisindole alkaloids from *Leuconotis griffithii*. J Nat Prod 81:2600–2604
16. Nugroho AE, Hirasawa Y, Kaneda T, Shirota O, Morita H (2021) Triterpenoids from *Walsura trichostemon*. J Nat Med 75: 415–422
17. Hirasawa Y, Agawa-Kakimoto M, Zaima K, Uchiyama N, Goda Y, Morita H (2021) Complanadine F, a novel dimeric alkaloid from *Lycopodium complanatum*. J Nat Med 75:403–407
18. Nugroho AE, Ono Y, Jin E, Hirasawa Y, Kaneda T, Rahman A, Kusumawati I, Tougan T, Horii T, Zaini NC, Morita H, Tang Y, Nugroho AE, Hirasawa Y, Tougan T, Morita H (2021) Bisindole alkaloids from *Voacanga grandifolia* leaves. J Nat Med 75:408–414
19. Amelia P, Nugroho AE, Hirasawa Y, Kaneda T, Tougan T, Horii T, Morita H (2021) Two new bisindole alkaloids from *Tabernaemontana macrocarpa* Jack. J Nat Med 75:633–642
20. Spartan Software https://www.wavefun.com/products/spartan.html
21. TURBOMOLE GmbH (2019) TURBOMOLE V7.0, a development of University of Karlsruhe and Forschungszentrum Karlsruhe GmbH, 1989–2007. https://www.turbomole.org/
22. Asili J, Lambert M, Ziegler HL, Stærk D, Sairafianpour M, Witt M, Asghari G, Ibrahimi IS, Jaroszewski JW (2004) Labdanes and isopimaranes from *Platycladus orientalis* and their effects on erythrocyte membrane and on *Plasmodium falciparum* growth in the erythrocyte host cells. J Nat Prod 67:631–637
23. Trager W, Jensen JB (1976) Human malaria parasites in continuous culture. Science (80-) 193:673 LP – 675. https://doi.org/10.1126/science.781840
24. Lambros C, Vanderberg JP (1979) Synchronization of *Plasmodium falciparum* erythrocytic stages in culture. J Parasitol 65:418–420
25. Tougan T, Suzuki Y, Itagaki S, Izuka M, Toya Y, Uchihashi K, Horii T (2018) An automated haematology analyzer XN-30 distinguishes developmental stages of falciparum malaria parasite cultured in vitro. Malar J 17:59. https://doi.org/10.1186/s12936-018-2208-6
26. Toya Y, Tougan T, Horii T, Uchihashi K (2021) Lysercell M enhances the detection of stage-specific Plasmodium-infected red blood cells in the automated hematology analyzer XN-31 prototype. Parasitol Int 80:102206. https://doi.org/10.1016/j.parint.2020.102206
27. Tougan T, Toya Y, Uchihashi K, Horii T (2019) Application of the automated haematology analyzer XN-30 for discovery and development of anti-malarial drugs. Malar J 18:8. https://doi.org/10.1186/s12936-019-2642-0